Aging and Disease
www.aginganddisease.org
Early access date: December 15, 2025
http://dx.doi.org/10.14336/AD.2025.1221

Original Article

Single Cell RNAseq Analysis of Thyroid Hormone Effects on Retinal Glial Cells

Hongwei Ma[1], Shujuan Li[1], Yun Le[2], David Stanford[3], Willard M. Freeman[3, 4], Xi-Qin Ding[1*]

[1]Department of Cell Biology, University of Oklahoma Health Campus, Oklahoma City, Oklahoma 73104, USA. [2]Departments of Medicine Endocrinology, Cell Biology, and Ophthalmology, and Harold Hamm Diabetes Center, University of Oklahoma Health Campus, Oklahoma City, Oklahoma 73104, USA. [3]Genes & Human Disease Research Program, Oklahoma Medical Research Foundation, Oklahoma City, Oklahoma 73104, USA. [4]Veterans Affairs Medical Center, Oklahoma City, Oklahoma 73104, USA.

[Received September 27, 2025; Revised December 11, 2025; Accepted December 12, 2025]

ABSTRACT: Thyroid hormone (TH) signaling regulates cellular metabolism and stress response in the retina. Increased TH levels in circulation are associated with a higher incidence of age-related macular degeneration. Furthermore, stimulation of TH signaling induces retinal degeneration in mice, which is accompanied by the activation of retinal glial cells. Here, we investigated the transcriptional changes induced by triiodothyronine (T3) in retinal glial cells using single-cell RNA sequencing (scRNAseq) and bioinformatic analyses. One-month-old C57BL/6 mice were given T3 (20 µg/ml in drinking water) for four weeks, after which their retinal cells were collected to assess viability and undergo scRNAseq. The resulting data were analyzed using the Seurat package, visualized by the Loupe Browser, and Ingenuity Pathway Analysis. Analyses of differentially expressed genes (DEGs) in Müller cells, astrocytes, and microglia revealed significant enrichment in pathways associated with stress, immune response, and degeneration. Müller cells exhibited upregulation of mitochondrial dysfunction, acute-phase response, and sirtuin signaling pathways. Astrocytes displayed downregulation of synaptogenesis, neurovascular coupling, cAMP response elements, and calcium signaling. Microglia showed upregulation of coordinated lysosomal expression and regulation signaling, systemic lupus erythematosus in T cells, and multiple sclerosis signaling, and downregulation of actin-binding Rho activating signaling, retinoic acid receptor activation signaling, and IL-17 signaling. The distinct and overlapping transcriptional responses suggest that each retinal glial cell type plays a specific and coordinated role in adapting to stress. This study offers new insights into TH-induced retinal stress and degeneration at the transcriptional and pathway-level responses of retinal glial cells.

Keywords: Retina, Retinal glial cells, Müller cells, single-cell RNA sequencing, transcriptome, thyroid hormone

INTRODUCTION

Thyroid hormone (TH) signaling plays critical roles in cellular development, metabolism, and stress responses within the retina, and has been implicated in retinal cell survival and degeneration. Suppression of TH signaling with an anti-thyroid drug or targeting the intracellular TH components iodothyronine deiodinases and TH receptors protects retinal cells/photoreceptors in inherited [1-5] and induced [6, 7] mouse models of retinal degeneration, including age-related macular degeneration (AMD). Conversely, stimulation of TH signaling, either *via* triiodothyronine (T3) treatment [3, 8, 9] or deletion of T3-degrading enzymes [9], induces retinal degeneration. Furthermore, TH signaling has been associated with human retinal disease. Population and patient-based studies show that elevated TH signaling is associated with an increased incidence of AMD [10-20], and clinical evaluations revealed macular thinning in patients with thyroid-associated ophthalmopathy [21, 22].

***Correspondence should be addressed to:** Dr. Xi-Qin Ding, Department of Cell Biology, University of Oklahoma Health Campus, Oklahoma City, Oklahoma 73104, USA. E-mail: xi-qin-ding@ouhsc.edu.

TH signaling-induced retinal degeneration is characterized by activation of retinal glial cells [8, 23, 24]. In the retina, there are three types of glial cells: Müller cells, astrocytes, and microglial cells [25]. Müller cells and astrocytes are the primary macroglial cells in the retina, providing structural and functional support to retinal neurons and contributing to retinal homeostasis [25, 26]. Müller cells provide metabolic and neurotrophic support primarily to photoreceptors and secondary neurons. Astrocytes, on the other hand, primarily support retinal ganglion cells and maintain the structural and functional integrity of retinal vasculature. These cells exhibit activation and reactive gliosis under pathological conditions, characterized by morphological changes and upregulation of glial fibrillary acid protein (GFAP), which can have protective or detrimental effects depending on context [27]. Microglia are the primary immune cells residing in the retina. They are highly dynamic and crucial for immune surveillance and responding to injury and disease [28, 29]. Under normal conditions, microglia help maintain retinal structure and function *via* immune surveillance. In response to injury, infection, or disease, microglia become activated and initiate inflammatory responses, including changes in their morphology, proliferation, and migration to the site of injury, release of various inflammatory mediators that can either be protective or contribute to neuronal damage depending on the context and duration of activation. The ionized calcium-binding adaptor molecule 1 (IBA1) is a reliable marker for microglia, particularly when they are activated [30] . Our previous studies have shown that treatment with T3 increased the expression/upregulation of GFAP [8, 23, 24], indicating activation of Müller cells and astrocytes, and the expression/upregulation of IBA1 [24], indicating activation of microglia.

This study investigated the transcriptomic alterations in retinal Müller, astrocytes and microglial cells after T3 treatment using single-cell RNA sequencing (scRNAseq) and Ingenuity Pathway Analysis (IPA). We identified differential gene expression patterns among retinal glial cells, altered canonical pathways, and causal network changes within these cell types. We also found significant enrichment among differentially expressed genes (DEGs) in stress, immune response, and degeneration pathways in the glial cells. Comparative analysis highlighted both unique and shared transcriptional responses across the three glial cell types, supporting the interconnective regulatory networks between retinal support and immune cells. Findings from this study shall provide significant insights into the impacts of TH signaling on retinal glial cell activity and advance the understanding of TH-induced retinal stress and degeneration.

MATERIALS AND METHODS

Animals and T3 administration

C57BL/6J mice were obtained from Jackson Laboratory and maintained under a 12-hour light-dark cycle. Cage lighting during the light period was set to 7 foot-candles. All procedures for animal care and experimentation received approval from the Institutional Animal Care and Use Committee at the University of Oklahoma Health Campus, adhering to the guidelines of the Society for Neuroscience and the Association for Research in Vision and Ophthalmology. Mice received T3 (Sigma-Aldrich, T2877, St. Louis, MO, USA) through drinking water (20 µg/ml) for 4 weeks. The T3 drinking water was prepared by first dissolving 10 mg of T3 in 1.0 mL of 1.0 N NaOH and diluting with tap water to the final volume of 500 ml, as described previously [31, 32]. The 20 µg/ml T3 dose was selected based on the results from our previous dose-response investigations. In our dose-response studies, T3 administered at this concentration was shown to induce significant morphological and functional alterations in the retina [8]. Control mice received regular tap water. Both male and female mice were included.

Retinal extraction and cell dissociation

Retinas were isolated from the eyes of both control and T3-treated mice and placed in Dulbecco's Modified Eagle Medium (ThermoFisher, Richardson, TX, USA). One retina was snap-frozen in liquid nitrogen and kept at −80 °C for RNA extraction, while the other retina underwent cellular dissociation using the Neural Tissue Dissociation Kit-Postnatal Neurons (Miltenyi Biotec, cat# 130-094-802). Retinal samples were rinsed twice in DPBS containing calcium, magnesium (Sigma-Aldrich, cat# D8662), and 0.5% BSA before adding 1960 µL of enzyme mix 1. Samples were incubated with gentle rotation at 37 °C for 15 minutes, followed by the addition of 30 µL of enzyme mix 2, gentle pipetting, and an additional 10-minute incubation. Another 15 µL of enzyme mix 2 was added, and retinal tissue was further dissociated by pipetting and filtered through a 70 µm SmartStrainer (Miltenyi Biotec, cat# 130-098-462). The cell suspension was centrifuged at 130× g for 10 minutes, followed by washing, filtering, and quantification. Cell viability was assessed via flow cytometry using propidium iodide (cat# 130-093-233, MACSQuant Analyzer cat# 130-096-343). Prior to loading for single-cell RNA sequencing (scRNAseq), cells were adjusted to 1000 cells/µL, targeting the recovery of 5000 cells per sample.

Library preparation and scRNAseq analysis

Single-cell RNA sequencing libraries were constructed using the Chromium Single Cell 3′ GEM, Library & Gel Bead Kit v3 (10× Genomics, cat# 10000075) as per the manufacturer's instructions. Cells, master mix, gel beads, and partitioning oil were loaded onto a Chromium Single Cell B Chip (10× Genomics, cat# 10000073) and processed on the Chromium Controller (10× Genomics, cat# 1000204) to generate gel beads-in-emulsion (GEMs) for library creation. GEMs were thermocycled for reverse transcription and cleaned with Dynabeads MyOne SILANE reagent. Amplified cDNA was purified using SPRISelect reagent beads (Beckman Coulter, cat# B23318) and checked for quality with a High Sensitivity D5000 ScreenTape on a TapeStation 2200 (Agilent, cat# G2964AA). Libraries were quantified by qPCR, normalized, pooled, and sequenced on an Illumina NovaSeq 6000 system (SP PE50bp, S4 PE150) with ~50,000 reads per cell.

Data processing and statistical analysis

Following sequencing, reads were trimmed and aligned, and differential expression statistics and correlation analyses were performed, as described previously [33]. Reads were mapped to the Mm10 mouse genome (2014.11.26). Cellranger mkfastq was utilized to demultiplex the fastq files, and Cellranger counts and Cellranger aggregates were used under default settings. Cells with high mitochondrial content were filtered, and clustering was performed using UMAP. Differential expressions were analyzed using Student's *t*-test, defining significant differences at $p < 0.05$. A fold-change threshold of >1.25 was applied to select biologically meaningful genes.

Cell identification and gene expression profiling

Cell types were identified using Loupe Browser (10× Genomics) based on gene expression patterns observed in UMAP and t-SNE plots. Marker genes for specific cell types include *Clue*, *Glul*, *Apoe*, *Rlbp1*, and *Crabp1* for Müller cells; *Gfap* and *Apoe* for astrocytes; and *C1qa*, *Tmem119*, *Aif1*, *Cd163*, and *Apoe* for microglia. Differential gene expressions were determined by comparing post-T3 treatment cell types, with a significance threshold of $p < 0.05$.

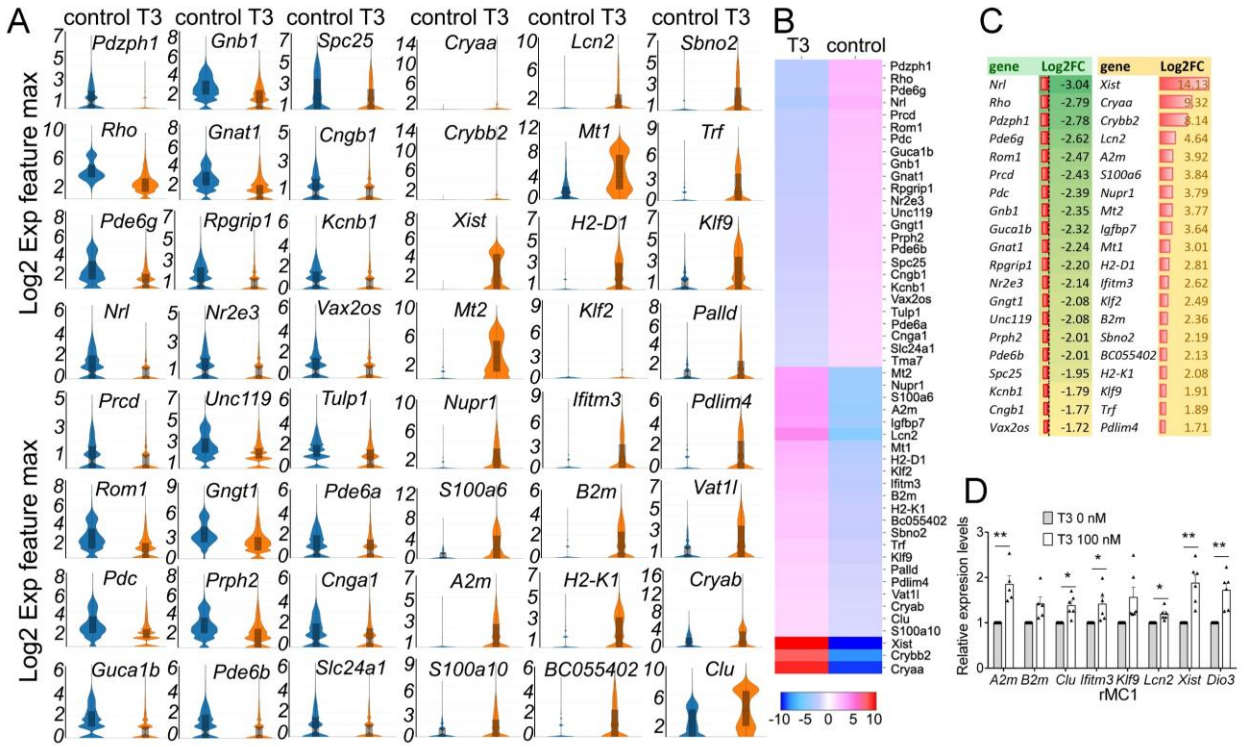

Figure 1. Transcriptomic profiles of Müller cells in mouse retina after T3 treatment. (**A**) Violin plots from scRNAseq showing the expression profiles of representative genes in Müller cells from control and T3-treated mice. (**B**) Heat map displaying the top 50 differentially expressed genes (DEGs) in Müller cells after T3 treatment. (**C**) Bar chart showing the top 20 upregulated and downregulated DEGs in Müller cells following T3 treatment. (**D**) qRT-PCR validation of gene expression profiles in Müller cells after 48 hours of T3 treatment. Experiments were conducted in triplicate, with each experiment including two biological replicates. Gene expression levels were normalized to those of untreated rMC1 cells. Data are presented as mean ± SEM from 4 individual mice per group (**A-C**) and 3 independent experiments (**D**) (*p<0.05, ** p<0.01).

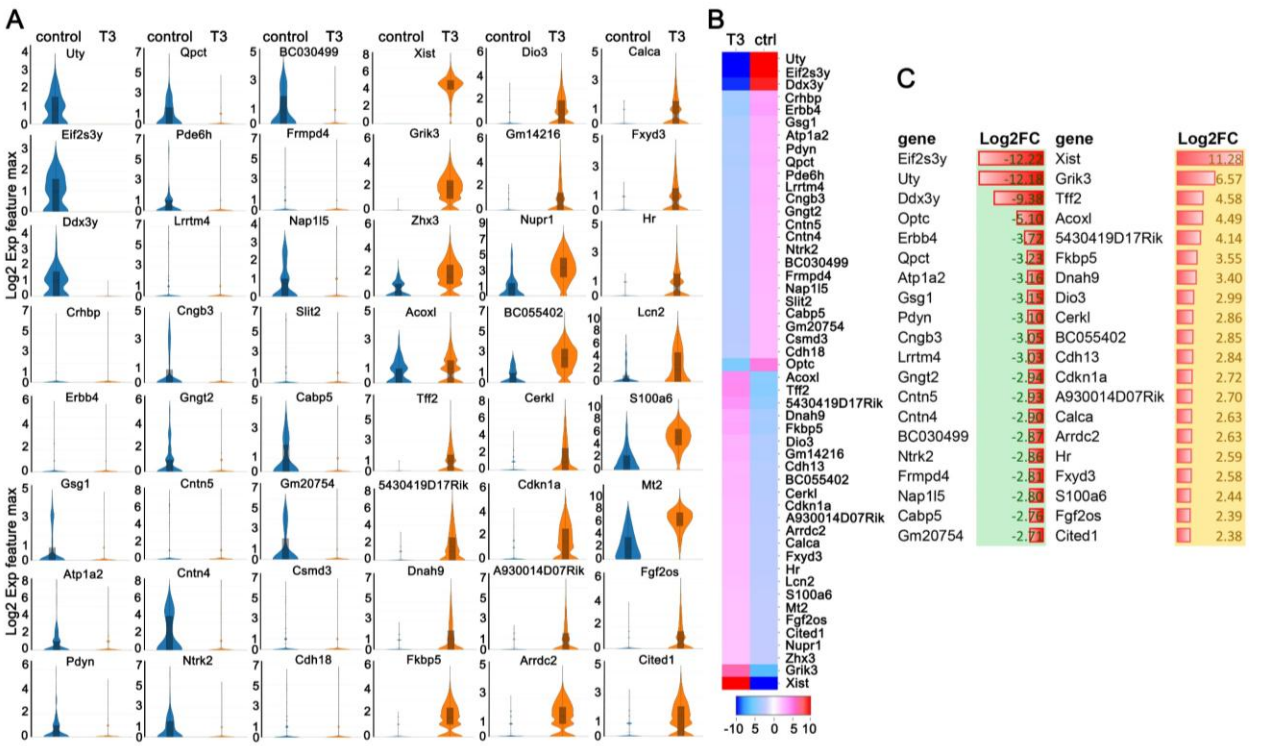

Figure 2. Transcriptomic profiles of astrocytes in mouse retina after T3 treatment. (**A**) Violin plots from scRNAseq showing expression profiles of representative genes in astrocytes from control and T3-treated mice. (**B**) Heat map of the top 50 DEGs in astrocytes after T3 treatment. (**C**) Bar chart showing the top 20 upregulated and downregulated DEGs in astrocytes following T3 treatment.

Pathway analysis

Ingenuity Pathway Analysis (IPA, Qiagen) was utilized to identify key canonical pathways, upstream regulators, and associated diseases and functions within the dataset.

Cell culture

The rat Müller cell line, rMC1, was provided by Dr. Vijay P. Sarthy at Northwestern University [34]. These cells were cultured in DMEM medium with 4.5 g/L glucose (Gibco, Cat#: 11965-092), supplemented with 10% fetal bovine serum (Gibco, Cat#: 10438026) and 1% penicillin–streptomycin (Gibco, Cat#: 15140122). For experimental purposes, cells were seeded at a concentration of 1×10^5 cells per well in a 6-well plate and incubated overnight. After 16 hours, cells were treated with culture medium containing 0, 10, or 100 nM T3 and incubated for an additional 24 or 48 hours. At the end of the incubation period, the medium was removed, and cell lysis buffer was added to each well for RNA isolation.

RNA extraction and qRT-PCR

Total RNA was isolated from the retinas using the PureLink RNA Mini Kit (ThermoFisher, cat# 12183018A). Reverse transcription was carried out with iScript Reverse Transcription Supermix for qRT-PCR (Bio-Rad, cat# 1708841). *Hprt1* was used as an internal control, all genes were assessed in duplicate, and relative gene expression was calculated by the ΔΔCt method. The primers used are shown in Supplementary Table 1.

RESULTS

To study the transcriptomes of retinal cells following the stimulation of TH signaling, we performed droplet sequencing on retinas from control mice and mice treated with 20 μg/mL T3 *via* drinking water for four weeks. Retinas from four mice per group were dissociated, yielding an average cell viability of 57.5% as assessed by flow cytometry. Following preprocessing and quality control, 155,866 single cells were identified and grouped into 13 clusters. These cells, which included samples from both the control and T3-treated retinas, had a median count of 918 genes and 1,465 unique molecular identifiers (UMIs) per cell. Retinal glial cell clusters (Müller cells, astrocytes, and microglia) were annotated based on established marker genes. Cluster analysis identified 7,716 Müller cells (5.0%), 2,959 astrocytes (1.9%), and 808 microglia (0.5%) within the sample. T3 treatment induced substantial changes in gene expression across

these retinal glial cells. Specifically, 179 DEGs were detected in Müller cells (15.3%), 163 in astrocytes (14%), and 100 in microglia (8.6%). The overall clusters and cell type identification for the T3-treated retinas have been reported previously [35].

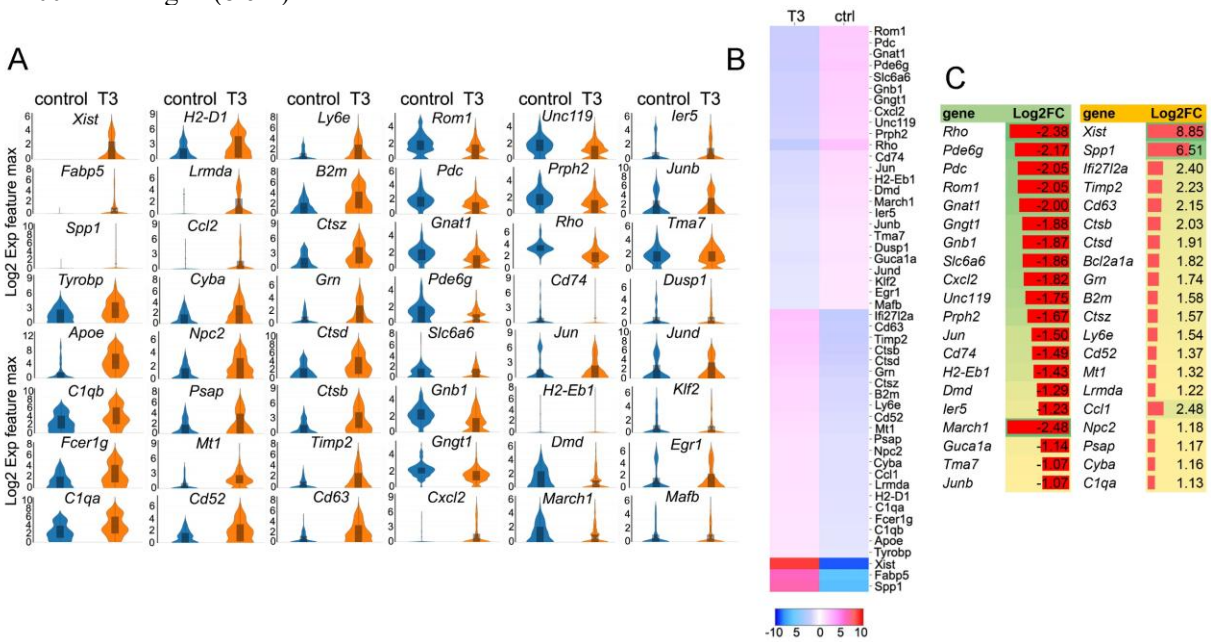

Figure 3. Transcriptomic profiles of microglia in mouse retina after T3 treatment. (**A**) Violin plots from scRNAseq showing expression profiles of representative genes in microglial cells from control and T3-treated mice. (**B**) Heat map of the top 50 DEGs in microglial cells after T3 treatment. (**C**) Bar chart showing the top 20 upregulated and downregulated DEGs in microglia following T3 treatment.

Transcriptomic profiles of retinal glial cells after T3 treatment

scRNA-seq analysis of the macroglial Müller cells revealed significant differential gene expression following T3 treatment. Violin plots showed the expression levels of key genes, highlighting both up- and down-regulated genes in T3-treated samples (Fig. 1A). A heat map further illustrated the top 25 up- and down-regulated genes (Fig. 1B). Key upregulated genes were associated with stress response (e.g., *Lcn2, A2m, S100a6, Nupr1*, and *Mt2*) and metabolic regulation (e.g., *Klf2, Klf9,* and *Igfbp7*), while downregulated genes were linked to cellular structure maintenance (e.g., *Rho, Rom1, Prph2, Rpgrip1, Cngb1,* and *Prcd*) (Fig. 1C). To validate the transcriptomic findings in Müller cells, we selected seven upregulated genes: *A2m*, *Clu*, *Ifitm3*, *Lcn2*, *Xist*, *B2m*, and *Kif9*, for verification of their response to T3 in a Müller cell line. The gene *Dio3*, which encodes the enzyme iodothyronine deiodinase 3, was included and served as a positive control. This enzyme inactivates T3 and is upregulated after T3 treatment [8]. Given the lack of an available mouse Müller cell line, we used a rat Müller cell line (rMC1), which closely resembles murine Müller cells in cellular characteristics. Two doses of T3 (10 nM and 100 nM) were used to evaluate its effects on the selected genes. We found that T3 treatment at 100 nM for 48 hours, but not at 10 nM, significantly increased the expression of six of the eight genes examined (*A2m*, *Clu*, *Ifitm3*, *Lcn2*, *Xist*, and *Dio3*) (Fig. 1D).

T3 treatment also induced distinct differential gene expression in astrocytes. The violin plots (Fig. 2A) and heat map (Fig. 2B) highlighted both upregulated and downregulated genes in T3-treated astrocytes. Key upregulated genes were associated with epigenetic regulation (*Xist*, *Fkbp5*, *Dio3*, *Cdh13*), neuronal & ciliary function (*Grik3*, *Dnah9*, *Cerkl*), and metabolic homeostasis (*Tff2*, *Acoxl*, *Dio3*), while downregulated genes were linked to neuropeptide & stress regulation (*Pdyn*, *Qpct*, *Atp1a2*) and protein quality control (*Uty*) (Fig. 2C).

Similar to the macroglial cells, microglial cells in the retina also exhibited differential gene expression in response to T3 treatment. Violin plots (Fig. 3A) and heat map (Fig. 3B) highlighted both upregulated and downregulated genes in T3-treated microglial cells. Key upregulated genes were associated with immune response (e.g., *B2m, C1qa, Ccl1, Spp1,* and *Ifi27l2a*) and phagocytosis (*Cyba, Cd63, Ctsb, Ctsd, Psap,* and *Npc2*), while key downregulated genes were associated with vision-specific retinal survival (*Rho*, *Pde6g*, *Rom1*, *Gnat1*, and *Slc6a6*) and neuroinflammation (*Cxcl2*) (Fig. 3C).

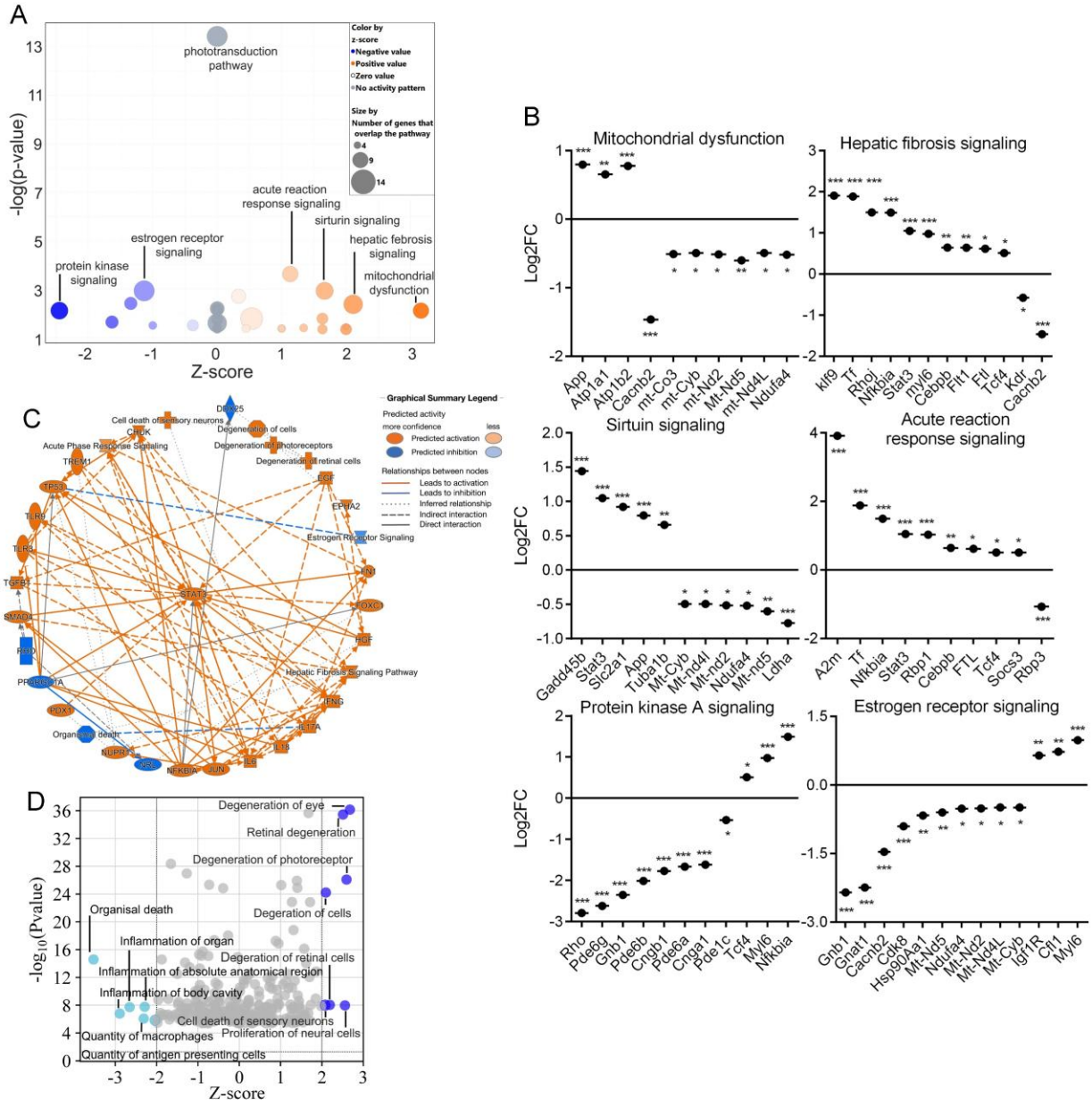

Figure 4. Canonical pathways and connections to function/disease in Müller cells after T3 treatment. (**A**) Bubble chart illustrating canonical pathways altered in Müller cells following T3 treatment, based on p-value, z-score, and the number of overlapping DEGs. (**B**) Shown are genes significantly altered in the pathways, as highlighted in (**A**). (**C**) Graphical summary depicting the connections between the pathway changes and diseases/functions. (**D**) Volcano plot of diseases and functions altered in Müller cells after T3 treatment, generated based on p-value and z-score.

Canonical pathways and connections to function/disease in retinal glial cells after T3 treatment

Pathway alterations in Müller cells after T3 treatment were identified *via* the IPA analysis. As visualized by bubble charts and volcano plots, notable impacted pathways included mitochondrial dysfunction, hepatic fibrosis signaling, sirtuin signaling, acute response signaling, protein kinase signaling, and the estrogen receptor signaling (Fig. 4A-B). The graphical summary highlighted the connections between these pathways and cellular degeneration/inflammation, including degeneration of cells, degeneration of photoreceptors, degeneration of retinal cells, hepatitis fibrosis signaling pathways, acute phase response signaling, and cell death of sensory neurons (Fig. 4C-D). Diseases and Functions Analysis (DFA) in IPA links the gene expression data to known biological functions, diseases, and disorders. It

assesses whether specific biological processes or diseases are predicted to be altered based on the genes in the dataset. DFA of Müller cells showed that T3 treatment altered their function and pathophysiological activity. The treatment enhanced retinal and photoreceptor cell death/degeneration, including degeneration of the eye (Supplementary Fig. 1A), degeneration of photoreceptors (Supplementary Fig. 1B), retinal degeneration (Supplementary Fig. 1C), cell death of sensory neurons (Supplementary Fig. 1D), degeneration of retinal cells (Supplementary Fig. 1E), and degeneration of cells (Supplementary Fig. 1F). The treatment also weakened the inflammatory response pathways, including quantity of macrophages (Supplementary Fig. 1G), organismal death (Supplementary Fig. 1H), inflammation of anatomical regions (Supplementary Fig. 1I), inflammation of organs (Supplementary Fig. 1J), and inflammation of body cavities (Supplementary Fig. 1K).

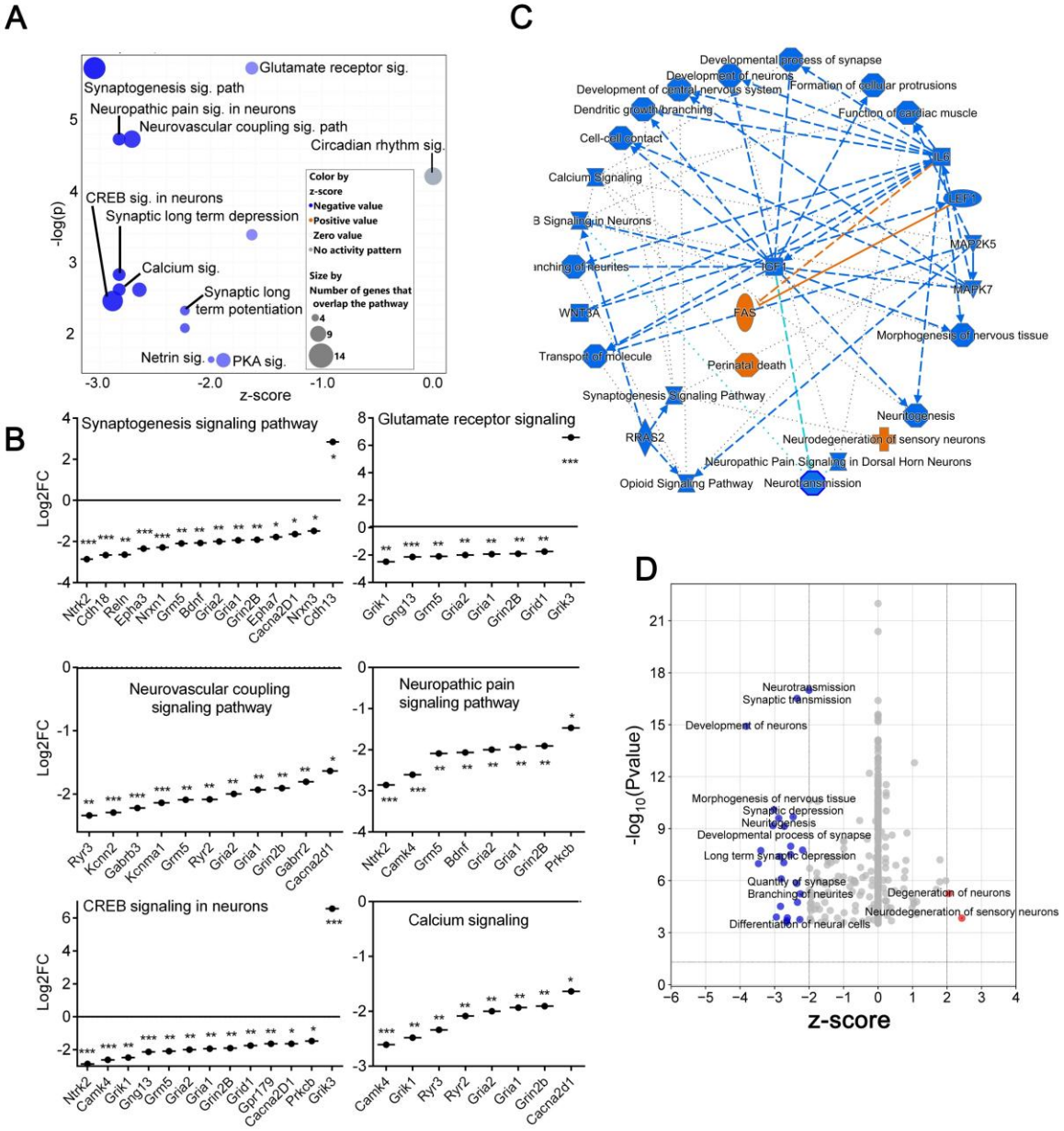

Figure 5. Canonical pathways and connections to function/disease in astrocytes after T3 treatment. (**A**) Bubble chart displaying canonical pathways altered in astrocytes after T3 treatment, generated based on p-value, z-score, and DEG overlap. (**B**) Shown are significantly altered genes in the pathways, as indicated in (**A**). (**C**) Graphical summary of T3-treated astrocytes showing connections between the pathway changes and diseases/functions. (**D**) Volcano plot of altered diseases and functions in astrocytes after T3 treatment, based on p-value and z-score.

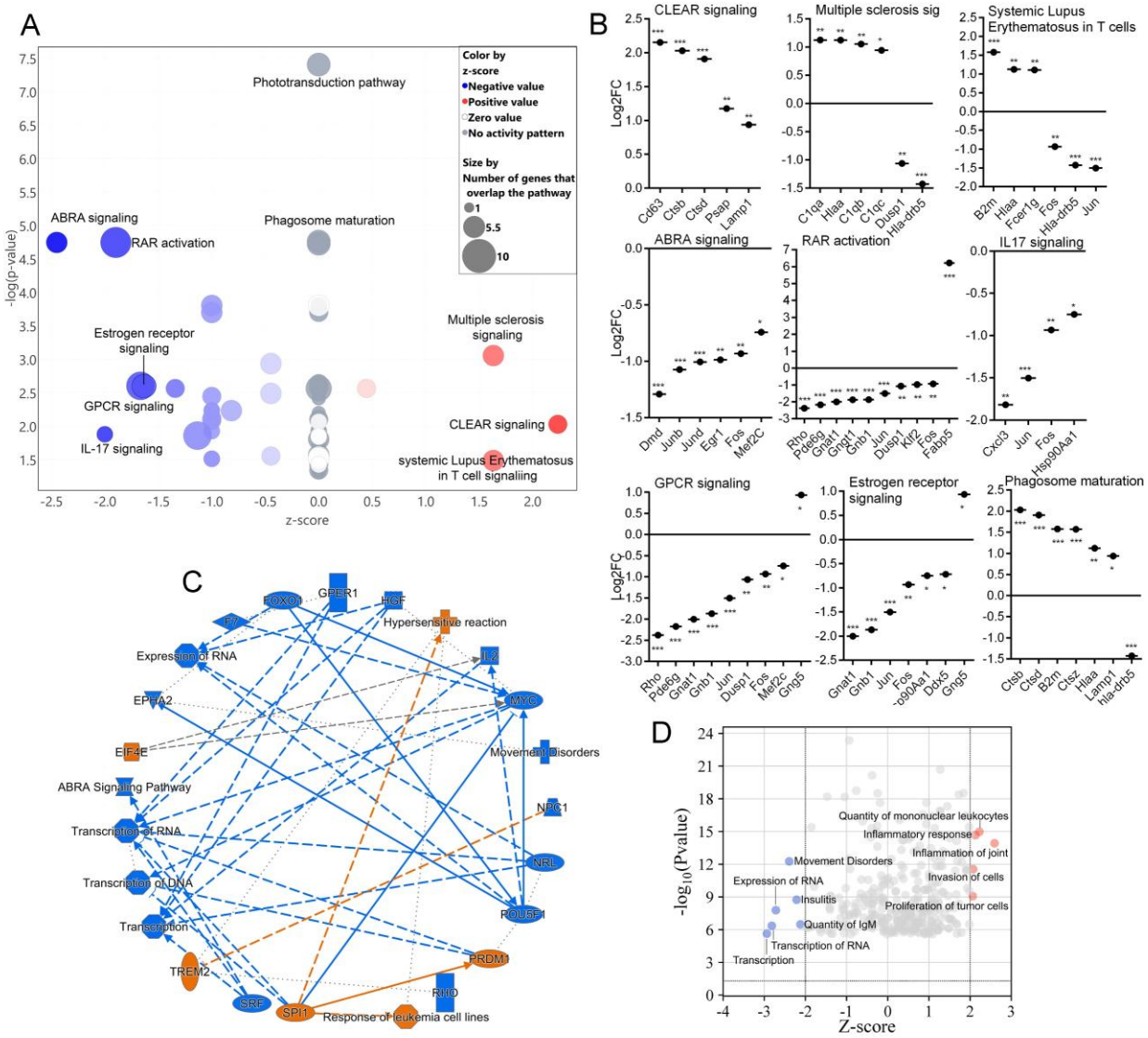

Figure 6. Canonical pathways and connections to function/disease in microglia after T3 treatment. (**A**) Bubble chart displaying canonical pathways altered in microglial cells after T3 treatment, generated based on p-value, z-score, and DEG overlap. (**B**) Shown are genes significantly altered in pathways, as indicated in (**A**). (**C**) Graphical summary of T3-treated microglial cells showing connections between the pathway changes and diseases/functions. (**D**) Volcano plot of altered diseases and functions in microglial cells after T3 treatment, based on p-value and z-score.

Pathway analysis of astrocytes revealed downregulation of synaptogenesis signaling, glutamate receptor signaling, neuropathic pain signaling, neurovascular-coupling signaling pathways, cAMP response element-binding protein signaling (Fig. 5A-B). A number of connections are evident between downregulation of these pathways and the cellular activities in neurogenesis, neurotransmission, morphogenesis of nervous tissue, transport of molecules, cell-cell contact, dendritic growth/branching, development of neurons, and developmental process of synapses in astrocytes (Fig. 5C-D). DFA of astrocytes showed that specific functions, including molecular transport (Supplementary Fig. 2A), neurotransmission (Supplementary Fig. 2B), neuronal development (Supplementary Fig. 2C), neurogenesis (Supplementary Fig. 2D), synaptic transmission (Supplementary Fig. 2E), formation of cellular protrusions (Supplementary Fig. 2F), nervous tissue morphogenesis (Supplementary Fig. 2G), and cell-cell contact (Supplementary Fig. 2H), were downregulated after T3 treatment. In contrast, functions associated with motor dysfunction/movement disorders (Supplementary Fig. 2I), neuronal degeneration (Supplementary Fig. 2J), and sensory neuron neurodegeneration (Supplementary Fig. 2K), were upregulated.

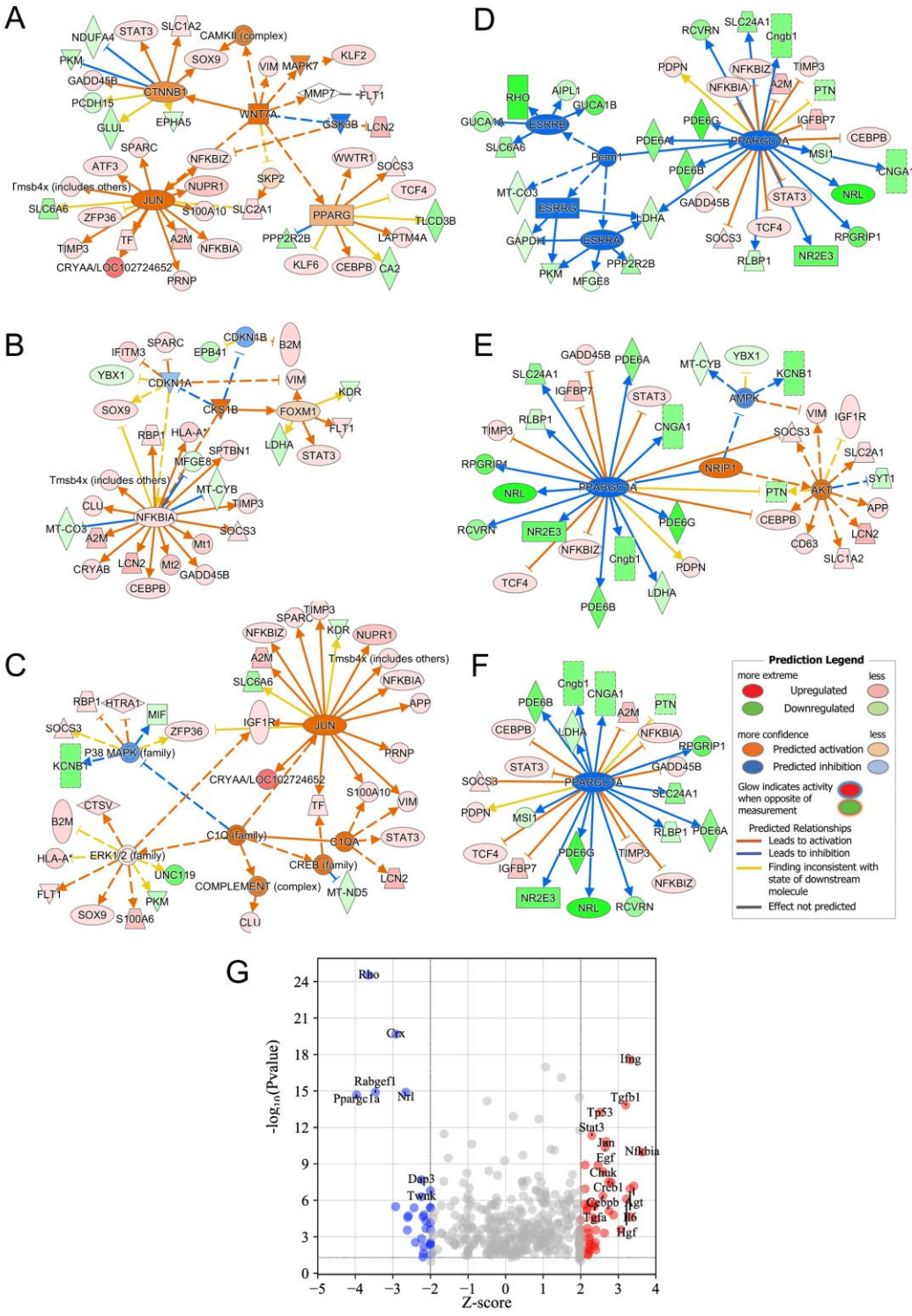

Figure 7. Causal networks and potential upstream regulators in Müller cells after T3 treatment. (**A**) Upregulated networks centered around Ctnnb1, Wnt7a, Pparg, and Jun. (**B**) Upregulated networks centered around Cks1b, Nfkbia, Foxm1, and Cdkn1a. (**C**) Upregulated networks centered around C1q family, Jun, C1qa, Mapk, and Erk1/2, and downregulated network centered around P38 Mapk family. (**D**) Downregulated networks centered around Perm1 and Ppargc1a. (**E**) Downregulated network centered around Ppargc1a and upregulated network centered around Akt. (**F**) Detailed focus on the downregulation of Ppargc1a. (**G**) Volcano plot of upstream regulators altered in Müller cells after T3 treatment, with colored regulators indicating both significant p-values and z-scores.

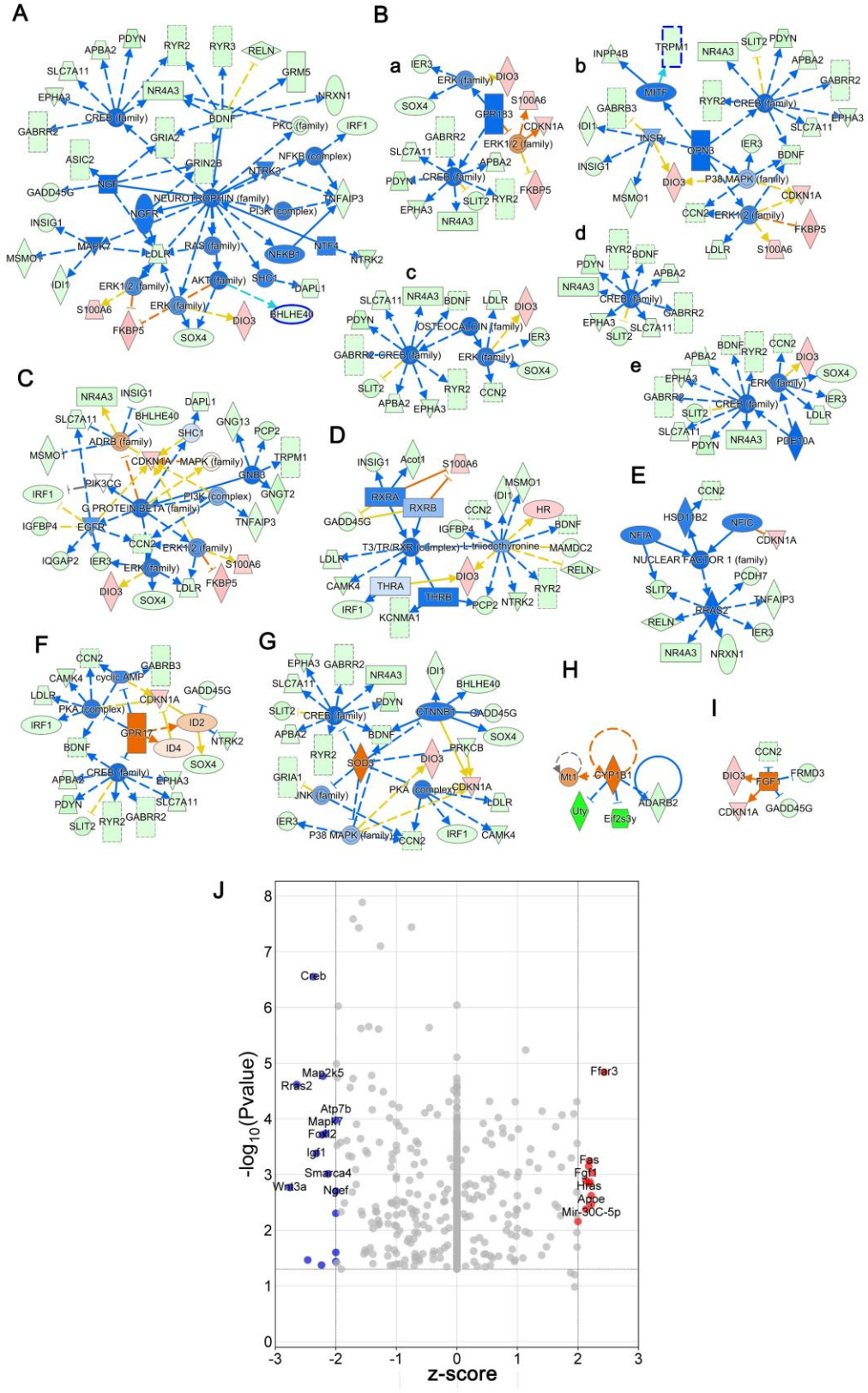

Figure 8. Causal networks and potential upstream regulators in astrocytes after T3 treatment. (**A**) Downregulated networks centered around Creb, neurotrophin, and Bdnf. (**B**) Downregulated networks centered around Creb. (**C**) Downregulated networks centered around G-protein β family. (**D**) Downregulated

networks centered around T3/TR/RXR. (**E**) Downregulated networks centered around Rras2 and nuclear factor 1. (**F**) Upregulated network centered around Gpr17, and downregulated networks centered around Creb and Pka. (**G**) Upregulated network centered around Sod3, and downregulated networks centered around Creb, Pka, and Ctnnb1. (**H**) Upregulated network centered around Cyp1b1. (**I**) Upregulated network centered around Fgf1. (**J**) Volcano plot of upstream regulators altered in astrocytes after T3 treatment, with colored regulators indicating both significant p-values and z-scores.

Pathway analysis of microglial cells revealed upregulation of coordinated lysosomal expression and regulation signaling, systemic lupus erythematosus in T cells, and multiple sclerosis signaling, and downregulation of actin-binding Rho activating signaling, retinoic acid receptor signaling, estrogen receptor signaling, G protein-coupled receptor signaling, and IL-17 signaling (Fig. 6A-B). Alteration of these pathways and cellular degeneration and inflammation, including degeneration of cells, degeneration of photoreceptors, degeneration of retinal cells, hepatitis fibrosis signaling pathways, acute phase response signaling, and cell death of sensory neurons are also predicted based on the gene expression patterns (Fig. 6C-D). DFA of microglial cells also revealed that inflammation and phagocyte activation were activated after T3 treatment, including quantity of mononuclear leukocytes (Supplementary Fig. 3A), activation of phagocytes (Supplementary Fig. 3B), inflammation of joint (Supplementary Fig. 3C), and proliferation of tumor cells (Supplementary Fig. 3D). Downregulation of RNA transcription (Supplementary Fig. 3E), transcription (Supplementary Fig. 3F), RNA expression (Supplementary Fig. 3G), movement disorders (Supplementary Fig. 3H), and IgM quantity (Supplementary Fig. 3I) was observed in microglial cells after T3 treatment.

Causal networks in retinal glial cells after T3 treatment

Causal Network Analysis (CNA) was then used to identify causal relationships and network of interconnected molecules and predict upstream regulators that are likely responsible for the observed gene expression changes in the dataset and provide potential mechanistic information. CNA of Müller cells revealed that upregulated causal networks in Müller cells after T3 treatment centered on Jun, Wnt7a, Ctnnb1, Pparg, Nfkbia, Erk1/2, and Stat3 (Fig. 7A-C) and downregulated networks centered on Ppargc1a and Perm1 (Fig. 7D-F). The upstream regulators identified by CNA included Stat3, Nfκb, Jun, Il6, Ifng, Chuk, Trem1, Tp53, Tlr9, Tgfb1, and Egf (Fig. 7G).

CNA of astrocytes showed major downregulated nodes, including neurotrophin, *Creb,* G protein β, T3/Tr/Rxr, and *Nfi* (Fig. 8A-E), along with upregulated nodes such as *Gpr17, Sod3, Cyp1b1,* and *Fgf1* (Fig. 8F-I). CNA also identified several key upstream regulators that were downregulated, including *Creb, Map2k5, Rras2, Atp7b, Mapk7, Foxl2, Igf1, Smarca4, Wnt3a,* and *Ngef,* as well as upregulated regulators such as *Ffar3, Fas, Fgf1, Hras, Apoe,* and *miR-30C-5p* (Fig. 8J).

CNA of microglial cells showed key upregulated nodes such as Akt, Sod, Fbxw7, and Eif4e in these cells (Fig. 9, A-D), and downregulated nodes, including 26S proteasome, Nfkb, Tnfrsf12a, Rho, and Npc1 (Fig. 9A-B, E-F). CNA also identified the upstream regulators involved in the disease pathways, including upregulated regulators Chuk, Trem2, Spi1, Ifna2, Akt, Eif4e, Sod, and Fbxw7, and downregulated regulators Rho, Abr, Npc1, Tnfrsf12a, Nfkb, Epha2, and Gper1 (Fig. 9G).

Comparative analysis across retinal glial cell types

Comparative analysis of the DEGs identified in each cell type revealed 34 were common between Müller and microglial cells, 6 between Müller cells and astrocytes, and 1 between microglial cells and astrocytes (Supplementary Fig. 4A). Among the 34 DEGs shared between Müller and microglial cells, 9 were upregulated, 19 were downregulated, and 6 exhibited opposing expression patterns (Supplementary Fig. 4B). Among the 6 DEGs shared between Müller cells and astrocytes, 4 were upregulated and 2 were downregulated, with consistent expression directions (Supplementary Fig. 4C). Upregulation of lncRNA *Xist* (X-inactive specific transcript) was detected across all three retinal glial cell types. Müller cells and microglial cells also shared several common pathways, including protein kinase A signaling, hepatic fibrosis signaling, G protein-coupled receptor signaling, and signaling by Rho family GTPases (Supplementary Tables 2-3). However, Müller cells exhibited unique pathways absent in microglial cells, such as oxidative phosphorylation, mitochondrial dysfunction, and tRNA splicing. In contrast, microglial cells showed distinct pathways, including MIF regulation of innate immunity, production of nitric oxide and ROS in macrophages, pathogen-induced cytokine storm signaling, and PPAR signaling (Supplementary Tables 2-3). Conversely, Müller and astrocytes shared few common pathways, including protein kinase A signaling (Supplementary Tables 4-5), and astrocytes mainly showed distinct pathways, including synaptogenesis signaling pathway, neurovascular coupling signaling pathway, CREB signaling in neurons, and calcium signaling (Supplementary Tables 4-7).

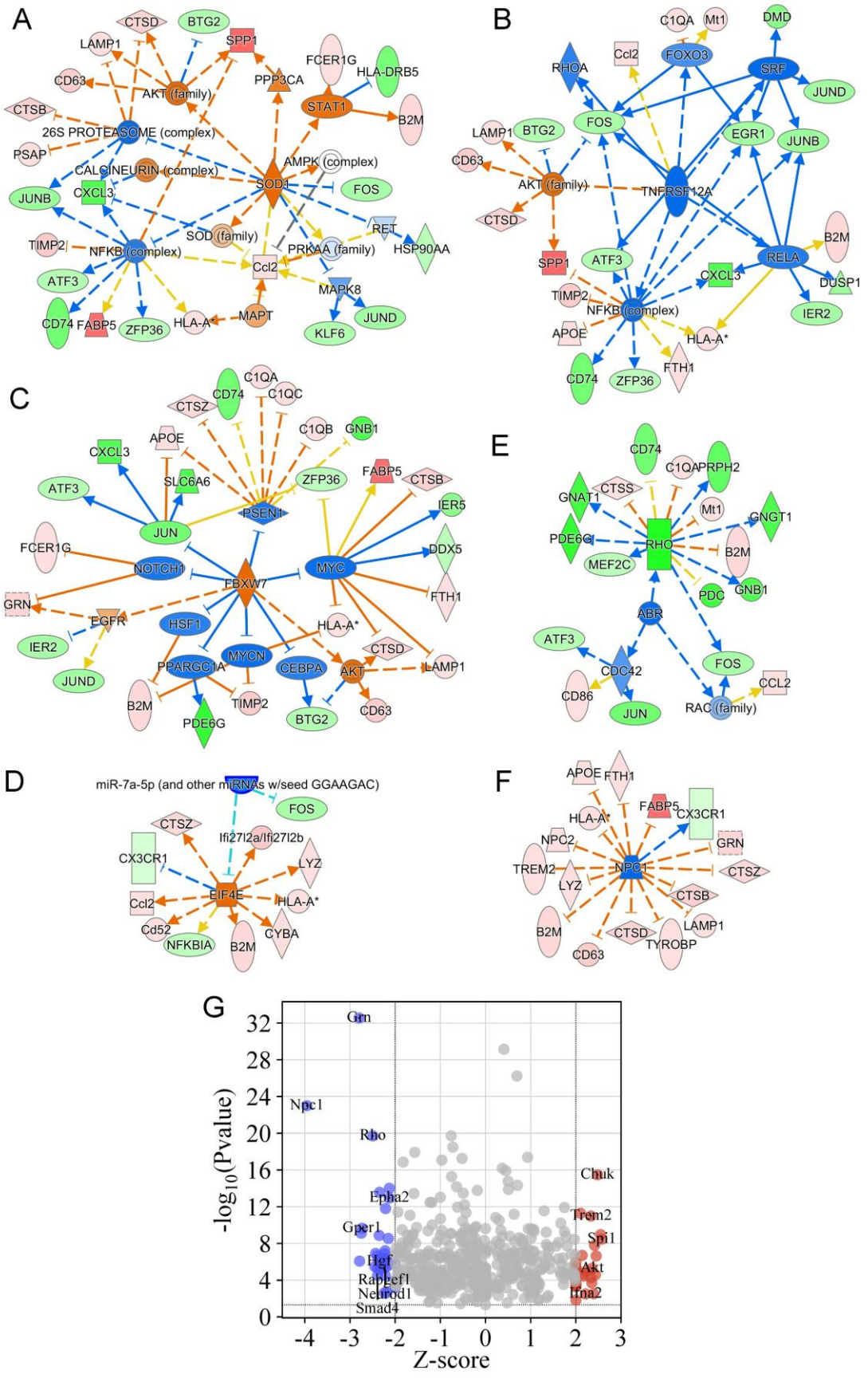
A
CTSD
BTG2
LAMP1
SPP1
FCER1G
HLA-DRB5
CD63
AKT (family)
PPP3CA
STAT1
B2M
CTSB
26S PROTEASOME (complex)
PSAP
CALCINEURIN (complex)
AMPK (complex)
SOD1
JUNB
CXCL3
FOS
RET
SOD (family)
TIMP2
NFKB (complex)
PRKAA (family)
HSP90AA
Ccl2
ATF3
MAPK8
CD74
FABP5
ZFP36
HLA-A*
MAPT
JUND
KLF6
B
C1QA
Mt1
DMD
Ccl2
FOXO3
RHOA
SRF
JUND
FOS
LAMP1
BTG2
EGR1
JUNB
CD63
AKT (family)
TNFRSF12A
CTSD
B2M
SPP1
ATF3
RELA
CXCL3
DUSP1
TIMP2
NFKB (complex)
IER2
APOE
HLA-A*
CD74
ZFP36
FTH1
C
C1QA
CD74
C1QC
CTSZ
C1QB
GNB1
APOE
CXCL3
SLC6A6
ZFP36
FABP5
CTSB
ATF3
PSEN1
IER5
JUN
FCER1G
DDX5
NOTCH1
MYC
FBXW7
FTH1
GRN
EGFR
HSF1
HLA-A*
IER2
MYCN
CTSD
PPARGC1A
CEBPA
AKT
LAMP1
JUND
B2M
TIMP2
CD63
PDE6G
BTG2
E
CD74
C1QAPRPH2
CTSS
GNAT1
Mt1
GNGT1
PDE6G
RHO
B2M
MEF2C
PDC
GNB1
ABR
ATF3
FOS
CDC42
CCL2
CD86
JUN
RAC (family)
D
miR-7a-5p (and other miRNAs w/seed GGAAGAC)
FOS
CTSZ
Ifi27l2a/Ifi27l2b
CX3CR1
LYZ
EIF4E
Ccl2
HLA-A*
Cd52
CYBA
NFKBIA
B2M
F
APOE
FTH1
HLA-A*
FABP5
CX3CR1
NPC2
GRN
TREM2
NPC1
CTSZ
LYZ
CTSB
B2M
CTSD
LAMP1
TYROBP
CD63
G
-log10(Pvalue)
Z-score
Grn
Npc1
Rho
Epha2
Gper1
Hgf
Rapgef1
Neurod1
Smad4
Chuk
Trem2
Spi1
Akt
Ina2

Figure 9. Causal networks and potential upstream regulators in microglia after T3 treatment. (**A**) Upregulated networks centered around Sod, Stat1, and Akt, and downregulated networks centered around Nfkb and 26S proteasome. (**B**) Upregulated network centered on Akt, and downregulated networks centered around Tnfrsf12a, Nfkb, Rela, Srf, and Foxo3. (**C**) Upregulated networks centered on Fbxw7 and Akt, and downregulated networks centered around Myc, Psen1, Notch 1, and Jun. (**D**) Upregulated network centered on Eif4e, and downregulated network centered on miR-7a-5p. (**E**) Downregulated networks centered around Rho, Abr, and Cdc42. (**F**) Downregulated network centered on Npc1. (**G**) Volcano plot of upstream regulators in microglial cells after T3 treatment, highlighting regulators with significant z-scores and p-values.

DISCUSSION

This work investigates transcriptional changes induced by T3 in retinal glial cells using scRNA-seq and bioinformatic analyses. It was built upon our previous work on scRNA-seq analysis of gene expression changes in mouse cone and rod photoreceptors after T3 treatment [35]. We extended this investigation to retinal glial cells. These cells account for approximately 7.4% of all sequenced retinal cells. Of these, Müller cells make up the majority (5.0%), followed by astrocytes (1.9%) and microglia (0.5%) [35]. From a total of 1,169 DEGs, Müller cells contribute 179 DEGs, astrocytes contribute 163, and microglia contribute 100 [35]. The retinal glial cells, which make up only 7.4% of the total sequenced cells, account for approximately 38% of all identified DEGs. This disproportionate representation suggests a high sensitivity of retinal glial cells to T3 treatment with significant transcriptomic alterations.

T3 treatment activates Müller cells

As major retinal supporting cells, Müller cells activate in response to stress, including T3 treatment, by upregulating GFAP expression [8, 23]. In line with these findings, this work demonstrates the activation of Müller cells after T3 treatment at the transcriptomic levels. This activation is marked by an increase in cellular and metabolic stress, mitochondrial dysfunction, and the activation of pathways related to inflammatory response/acute response signaling and sirtuin signaling. We have previously shown that the rod and cone photoreceptors also display mitochondrial dysfunction and oxidative stress after T3 treatment [35]. The results from Müller cells, along with the findings in photoreceptors, support the significant impact of TH signaling on mitochondrial function and metabolism in these cells. Similarly, the increase in acute response signaling transcriptional activity points toward an induction of cellular stress, inflammation, and potential pathology, in response to enhanced TH signaling. The increased sirtuin signaling transcriptional activity may reflect a neuroprotective and anti-inflammatory action of Müller cells in response to enhanced TH signaling. The response of Müller cells may reflect both the direct action of T3 and their reaction to stress in other retinal cells, like photoreceptors. The stress and degeneration of photoreceptors can, in turn, activate Müller cells.

It should be mentioned that Müller cells play a crucial role in the local regulation of TH signaling homeostasis under normal conditions. They achieve this through the action of the type 2 deiodinase (Dio2) enzyme, which converts the inactive hormone thyroxine (T4) into the active hormone T3 [36-38]. This local T3 production by Müller cells is essential for various retinal functions, including light adaptation and maintaining photoreceptor function [36]. Single-cell profiling shows that Müller cells coordinate retinal intercellular communication during light and dark adaptation *via* TH signaling [36]. Furthermore, a recent study has demonstrated that glucose levels regulate TH signaling in Müller cells. Specifically, in MIO-M1 cells (a human Müller cell line), glucose treatment induces a dose-dependent upregulation of DIO3 and downregulation of DIO2 expression [39]. These enzymatic changes reduce local T3 levels, a condition that is suggested to be protective during the early stages of diabetic retinopathy, but also to increase cell vulnerability in the chronic phase [39].

T3 treatment inhibits astrocytes

Transcriptomic analysis demonstrates that T3 treatment leads to an overall inhibition of astrocytes. This is shown by reduced expression of genes associated with neuropeptide and stress regulation as well as protein quality control. This is also evidenced by downregulation of the pathways related to synaptogenesis signaling, glutamate receptor signaling, neuropathic pain signaling, neurovascular-coupling signaling pathways, and cAMP response element-binding (CREB) signaling. IPA further connects the alterations in these pathways to degeneration of neurons and sensory neurons, motor dysfunction/ movement disorders, and impaired neurotransmission. Notably, *CREB* emerges as a central node within multiple causal networks, suggesting its critical role in astrocyte function following T3 treatment. This finding is consistent with previous findings showing TH signaling regulates astrocytic function and inhibits CREB activity [40, 41]. The reduced CREB signaling following T3 treatment may lead to the disruption of the neuroprotective, metabolic, and homeostatic functions of these cells. Inhibition of retinal astrocyte activity more

likely results from a direct effect of T3 on these cells rather than an indirect effect of degenerating photoreceptors, because astrocytes are primarily located in the inner retina near the retinal ganglion cells and do not directly contact photoreceptors in the outer retina. However, an indirect effect mediated by Müller cells, which span the whole retina and interact with both astrocytes and photoreceptors cannot be ruled out.

Similar to Müller cells, astrocytes also increase GFAP expression in response to stress [42, 43]. Given the overall inhibition of astrocytes after T3 treatment, the observed increase in GFAP expression in the mouse retina after T3 treatment is more likely from activated Müller cells than from astrocytes, though a co-immunolabeling of GFAP with markers for each cell type will provide more definitive evidence.

T3 treatment activates microglia

Transcriptomic analysis revealed that T3 treatment significantly impacts microglial cells. It activates these cells by upregulating genes and activating pathways that are key for immune response, immune vigilance, inflammatory response, neuro-inflammatory responses, and phagocytosis. Treatment with T3 activates microglia also by downregulating a variety of the genes that are linked to vision-specific retinal survival, actin-binding Rho activating signaling, retinoic acid receptors activation, estrogen receptor signaling, G protein-coupled receptor signaling, and IL-17 signaling. IPA further connects the alterations of these pathways to increased inflammation and phagocyte activation. Network analysis implies the significant immune regulatory role of microglia, with the Akt and NF-κB pathways at the center of their response, mediating T3-induced inflammation and stress. The calcium-binding protein IBA1 plays a key role in microglia motility, phagocytosis, and morphological changes; its expression is often upregulated when microglia are activated. We have previously shown the increased expression of IBA1 in the mouse retina after T3 treatment [24]. The transcriptomic analysis further demonstrated the activation of microglial cells at the gene expression levels. The data from microglia support a significant regulatory role of T3 in these cells.

T3 treatment induces shared and distinct response across retinal glial cell types

Retinal glial cells exhibit unique yet overlapping alterations of signaling in response to T3 treatment. Müller cells share more DEGs and pathway activities with microglial cells than with astrocytes. This suggests a greater degree of shared activity between Müller cells and microglia, while astrocytes exhibit more unique responses. Pathways related to inflammation and stress responses are common between Müller and microglial cells, highlighting their unique susceptibility/activation to TH stimulation. Through shared activities, these two cell types seem to synergistically manage cellular stress by altering their stress and inflammatory responses. A significant distinction in pathway alterations after T3 treatment is also present across retinal glial cell types, which supports the view that each plays a specialized, though interconnected role in preserving retinal integrity. Specifically, astrocytes display an overall inhibition with more unique alterations of the cellular signaling. The distinct and overlapping transcriptional responses observed among the retinal glial cells suggest interconnective regulatory networks exist between retinal support and immune cells. Furthermore, this data supports the view that each retinal glial cell type plays a specific and coordinated role in adapting to stress.

It is worth mentioning that the upregulation of lncRNA *Xist* (X-inactive specific transcript) is present across all three retinal glial cell types. The upregulation of this gene has also been detected in rod and cone photoreceptors after T3 treatment [35]. *Xist*'s canonical role is in X-chromosome inactivation. It can also act as a competing endogenous RNA [44], interacting with numerous microRNAs (miRNAs) to influence downstream gene expression [45, 46]. Nevertheless, recent research has uncovered its complex role in regulating inflammation, cell death, and proliferation across various cellular contexts [47, 48]. More specifically, *Xist* has been shown to restrain the activation of Müller cells and inflammation in diabetic retinopathy. Overexpression of *Xist* inhibits high glucose-induced activation of mouse and human retinal Müller cells and reduces the production of pro-inflammatory cytokines [49]. *Xist* has also been linked to retinoblastoma. Overexpression of *Xist* has been shown in retinoblastoma [50], while knockdown of *Xist* suppresses cell growth and proliferation in this tumor [51-54]. The upregulation of *Xist* across all retinal glial cell types suggests a potential common function of *Xist* in the retina under TH-induced stress and degeneration. The significance of this upregulation remains to be understood and merits further investigation.

Possible sex-specific effects

Both male and female mice were included in this study (n=4 per experimental condition, 2 males and 2 females). We acknowledge that the small subgroup size (n=2 per sex) limits the power to draw a definitive conclusion regarding sex-specific effects. As TH signaling and retinal response may differ between male and female, a future

study with an appropriately powered sample size is warranted to fully evaluate the sex-specific effect of TH signaling on retinal responses.

Potential biological implications of the glial cell transcriptional changes after T3 treatment

This work demonstrates that Müller cells and microglial cells were overall activated after T3 treatment, while astrocytes were inhibited. The activation of Müller cells and microglial cells in response to T3 treatment is anticipated to have both protective and harmful effects on the retinal cells. Specifically, prolonged Müller cell activation in response to excessive TH signaling leads to downregulation of their normal homeostatic functions, and ultimately harms photoreceptors and other retinal neurons via release of cytokines and toxic accumulation of extracellular glutamate around retinal neurons. Likewise, the initial activation of microglial cells to TH stimulation is likely neuroprotective, while sustained activation can lead to the release of pro-inflammatory mediators and cytotoxic factors (such as reactive oxygen species), which directly harm photoreceptors and other retinal neurons. At the molecular levels, retinal glial cell activation is primarily characterized by oxidative stress, mitochondrial dysfunction, elevation of sirtuin signaling and inflammatory responses in Müller cells, alongside a robust immune and inflammatory response in microglial cells. Indeed, treatment with an antioxidant alleviates T3-induced retinal degeneration and reduces Müller cell activation [23]. It is suggested that activating sirtuin signaling and modulating the inflammatory response could offer retinal protection against TH signaling-induced damage.

Inhibition of retinal astrocyte activity may not directly and immediately contribute to TH signaling-induced photoreceptor degeneration because of their location in the retina. However, the loss of astrocyte function may indirectly accelerate photoreceptor degeneration through the mechanisms of neurovascular dysfunction and loss of inner retinal support, which degrades the overall retinal environment. Nevertheless, further investigation is needed to address the specific role of retinal glial cells in T3-induced retinal degeneration.

Future perspectives/therapeutic significance

Suppressing TH signaling with an anti-thyroid drug or targeting the intracellular TH components iodothyronine deiodinases and TH receptors has been shown to protect retinal cells/photoreceptors in inherited [1-5] and induced [6, 7] mouse models of retinal degeneration, including AMD. Decreased TH signaling has also been shown to accelerate the reinnervation of the optic tectum after optic nerve crush in adult zebrafish [55]. The eye's accessibility to topically delivered therapeutics (eye drops) [56, 57] offers a significant advantage for disease management. This allows for the local inhibition of TH signaling at various levels, such as by targeting TH receptors or enzymes that regulate T3 levels in local tissues, or a combination of both. Therefore, the ocular delivery of a TH inhibitor may represent a potential therapeutic intervention for managing retinal degeneration.

In summary, T3 treatment transcriptionally activates Müller cells and microglia while inhibiting astrocytes, leading to a significant enrichment in pathways of stress, immune response, and degeneration in retinal glial cells. Each of the three glial cell types responds uniquely to T3 stimulation, though Müller cells and microglia share significant responses. This suggests that each cell type plays a specific, coordinated role in adapting to stress. This work illustrates the transcriptional profiles and relevant pathway alterations of retinal glial cells after TH signaling stimulation, offering new insights into TH-induced retinal stress and degeneration.

Data Availability Statement

The datasets generated and analyzed during the current study are available from the corresponding author upon reasonable request. All sequencing data have been deposited to Gene Expression Omnibus (GEO accession number: GSE313242).

Author Contribution

Xi-Qin Ding, Hongwei Ma, and Willard Freeman: Research design and supervision; Hongwei Ma, Shujuan Li, and David Stanford: Study execution and data curation; Yun Le and Willard Freeman: Resources; Hongwei Ma: Manuscript drafting; Xi-Qin Ding, Willard Freeman, Hongwei Ma, Shujuan Li, and Yun Le: Manuscript review and editing; Xi-Qin Ding, Willard Freeman, and Yun Le: Funding acquisition.

Acknowledgements

This work was supported by the National Eye Institute of the National Institutes of Health under grant numbers R01EY033841, R01EY26970, R01EY034946, P30EY 021725, P30AG050911, and P30GM122744. The research reported in this publication was also supported by the Oklahoma Center for the Advancement of Science and Technology and the Presbyterian Health Foundation.

Competing Interests

The authors declare that they have no competing interests.

Supplementary Materials

The Supplementary Data are submitted along with the main text of the manuscript.

Supplementary Materials

The Supplementary data can be found online at: www.aginganddisease.org/EN/10.14336/AD.2025.1221.

References

[1] Yang F, Ma H, Boye SL, Hauswirth WW, Ding XQ (2018). Overexpression of Type 3 Iodothyronine Deiodinase Reduces Cone Death in the Leber Congenital Amaurosis Model Mice. Adv Exp Med Biol, 1074:125-131.

[2] Yang F, Ma H, Butler MR, Ding XQ (2018). Deficiency of type 2 iodothyronine deiodinase reduces necroptosis activity and oxidative stress responses in retinas of Leber congenital amaurosis model mice. FASEB J, 32:fj201800484RR.

[3] Ma H, Thapa A, Morris L, Redmond TM, Baehr W, Ding XQ (2014). Suppressing thyroid hormone signaling preserves cone photoreceptors in mouse models of retinal degeneration. Proc Natl Acad Sci U S A, 111:3602-3607.

[4] Ma HW, Yang F, Butler MR, Belcher J, Redmond TM, Placzek AT, et al. (2017). Inhibition of thyroid hormone receptor locally in the retina is a therapeutic strategy for retinal degeneration. Faseb Journal, 31:3425-3438.

[5] Yang F, Ma H, Belcher J, Butler MR, Redmond TM, Boye SL, et al. (2016). Targeting iodothyronine deiodinases locally in the retina is a therapeutic strategy for retinal degeneration. Faseb j, 30:4313-4325.

[6] Ma H, Yang F, Ding XQ (2020). Inhibition of thyroid hormone signaling protects retinal pigment epithelium and photoreceptors from cell death in a mouse model of age-related macular degeneration. Cell Death Dis, 11:24.

[7] Ma H, Yang F, Ding XQ (2022). Deficiency of thyroid hormone receptor protects retinal pigment epithelium and photoreceptors from cell death in a mouse model of age-related macular degeneration. Cell Death Dis, 13:255.

[8] Ma H, Yang F, York LR, Li S, Ding X-Q (2023). Excessive Thyroid Hormone Signaling Induces Photoreceptor Degeneration in Mice. eneuro, 10:ENEURO.0058-0023.2023.

[9] Ng L, Lyubarsky A, Nikonov SS, Ma M, Srinivas M, Kefas B, et al. (2010). Type 3 deiodinase, a thyroid-hormone-inactivating enzyme, controls survival and maturation of cone photoreceptors. J Neurosci, 30:3347-3357.

[10] Chaker L, Buitendijk GH, Dehghan A, Medici M, Hofman A, Vingerling JR, et al. (2015). Thyroid function and age-related macular degeneration: a prospective population-based cohort study--the Rotterdam Study. BMC Med, 13:94.

[11] Gopinath B, Liew G, Kifley A, Mitchell P (2016). Thyroid Dysfunction and Ten-Year Incidence of Age-Related Macular Degeneration. Invest Ophthalmol Vis Sci, 57:5273-5277.

[12] Age-Related Eye Disease Study Research G (2000). Risk factors associated with age-related macular degeneration. A case-control study in the age-related eye disease study: Age-Related Eye Disease Study Report Number 3. Ophthalmology, 107:2224-2232.

[13] Lin SY, Hsu WH, Lin CL, Lin CC, Lin JM, Chang YL, et al. (2018). Evidence for an Association between Macular Degeneration and Thyroid Cancer in the Aged Population. Int J Environ Res Public Health, 15:902.

[14] Chatziralli I. MPG, Niakas D., Labiris G. (2017). Thyroidopathy and Age-Related Macular Degeneration: Is There Any Correlation. Biomed Hub 2:1-3.

[15] Xu Z, Zhang M, Zhang Q, Xu T, Tao L (2021). Thyroid Disease Is Associated with Higher Age-Related Macular Degeneration Risk: Results from a Meta-Analysis of Epidemiologic Studies. Ophthalmic Res, 64:696-703.

[16] Farvardin M, Mousavi SE, Zare K, Bazdar S, Farvardin Z, Johari M (2021). Thyroid Dysfunction as a Modifiable Risk Factor for Wet Type Age-Related Macular Degeneration: A Case-Control Study. J Curr Ophthalmol, 33:449-452.

[17] Li X, Li H, Cheng J, Wang M, Zhong Y, Shi G, et al. (2022). Causal Associations of Thyroid Function and Age-Related Macular Degeneration: A Two-Sample Mendelian Randomization Study. Am J Ophthalmol, 239:108-114.

[18] Abdelkader M, Abass N (2019). The Relation Between Age Related Macular Degeneration and Thyroid Disorders. International Journal of Ophthalmology & Visual Science, 4:101-105.

[19] Nicolini G, Casini G, Posarelli C, Amato R, Lulli M, Balzan S, et al. (2024). Thyroid Hormone Signaling in Retinal Development and Function: Implications for Diabetic Retinopathy and Age-Related Macular Degeneration. International Journal of Molecular Sciences, 25:7364.

[20] Hung SH, Xirasagar S, Kuang TT, Chang WW, Cheng YF, Kuo NW, et al. (2022). Association of Age-Related Macular Degeneration with Prior Hyperthyroidism and Hypothyroidism: A Case-Control Study. J Pers Med, 12:602.

[21] Blum Meirovitch S, Leibovitch I, Kesler A, Varssano D, Rosenblatt A, Neudorfer M (2017). Retina and Nerve Fiber Layer Thickness in Eyes with Thyroid-Associated Ophthalmopathy. Isr Med Assoc J, 19:277-281.

[22] Sayin O, Yeter V, Ariturk N (2016). Optic Disc, Macula, and Retinal Nerve Fiber Layer Measurements Obtained by OCT in Thyroid-Associated Ophthalmopathy. J Ophthalmol, 2016:9452687.

[23] Li S, Ma H, Ding XQ (2025). Resveratrol Protects Photoreceptors in Mouse Models of Retinal Degeneration. Antioxidants (Basel), 14:154.

[24] Li S, Ma H, Yang F, Ding X-Q (2025). Stimulation of Thyroid Hormone Signaling Induces Stress Responses in Mouse Retina. Adv Exp Med Biol 1468:273-277.

[25] Reichenbach A, Bringmann A (2020). Glia of the human retina. Glia, 68:768-796.
[26] Bringmann A, Pannicke T, Grosche J, Francke M, Wiedemann P, Skatchkov SN, et al. (2006). Müller cells in the healthy and diseased retina. Prog Retin Eye Res, 25:397-424.
[27] Vecino E, Rodriguez FD, Ruzafa N, Pereiro X, Sharma SC (2016). Glia–neuron interactions in the mammalian retina. Progress in Retinal and Eye Research, 51:1-40.
[28] Fontainhas AM, Wang M, Liang KJ, Chen S, Mettu P, Damani M, et al. (2011). Microglial Morphology and Dynamic Behavior Is Regulated by Ionotropic Glutamatergic and GABAergic Neurotransmission. PLOS ONE, 6:e15973.
[29] Liang KJ, Lee JE, Wang YD, Ma W, Fontainhas AM, Fariss RN, et al. (2009). Regulation of Dynamic Behavior of Retinal Microglia by CX3CR1 Signaling. Investigative Ophthalmology & Visual Science, 50:4444-4451.
[30] Lier J, Streit WJ, Bechmann I (2021). Beyond Activation: Characterizing Microglial Functional Phenotypes. Cells, 10:2236.
[31] Hamidi S, Aliesky H, Chen CR, Rapoport B, McLachlan SM (2010). Variable suppression of serum thyroxine in female mice of different inbred strains by triiodothyronine administered in drinking water. Thyroid, 20:1157-1162.
[32] East-Palmer J, Szkudlinski MW, Lee J, Thotakura NR, Weintraub BD (1995). A novel, nonradioactive in vivo bioassay of thyrotropin (TSH). Thyroid, 5:55-59.
[33] Isola JVV, Ocanas SR, Hubbart CR, Ko S, Mondal SA, Hense JD, et al. (2023). A single-cell atlas of the aging murine ovary. bioRxiv:2023.2004.2029.538828.
[34] Sarthy VP, Brodjian SJ, Dutt K, Kennedy BN, French RP, Crabb JW (1998). Establishment and characterization of a retinal Müller cell line. Investigative ophthalmology & visual science, 39:212-216.
[35] Ma H, Stanford D, Freeman WM, Ding XQ (2024). Transcriptomic Analysis Reveals That Excessive Thyroid Hormone Signaling Impairs Phototransduction and Mitochondrial Bioenergetics and Induces Cellular Stress in Mouse Cone Photoreceptors. Int J Mol Sci, 25:7435.
[36] Wei M, Sun Y, Li S, Chen Y, Li L, Fang M, et al. (2023). Single-cell profiling reveals Muller glia coordinate retinal intercellular communication during light/dark adaptation via thyroid hormone signaling. Protein Cell, 14:603-617.
[37] Trentin AG (2006). Thyroid hormone and astrocyte morphogenesis. J Endocrinol, 189:189-197.
[38] Arbogast P, Flamant F, Godement P, Glosmann M, Peichl L (2016). Thyroid Hormone Signaling in the Mouse Retina. PLoS One, 11:e0168003.
[39] Forini F, Nicolini G, Amato R, Balzan S, Saba A, Bertolini A, et al. (2024). Local modulation of thyroid hormone signaling in the retina affects the development of diabetic retinopathy. Biochim Biophys Acta Mol Basis Dis, 1870:166892.
[40] Mendez-Pertuz M, Sanchez-Pacheco A, Aranda A (2003). The thyroid hormone receptor antagonizes CREB-mediated transcription. EMBO J, 22:3102-3112.
[41] Dezonne RS, Stipursky J, Araujo AP, Nones J, Pavao MS, Porcionatto M, et al. (2013). Thyroid hormone treated astrocytes induce maturation of cerebral cortical neurons through modulation of proteoglycan levels. Front Cell Neurosci, 7:125.
[42] Wu KH, Madigan MC, Billson FA, Penfold PL (2003). Differential expression of GFAP in early v late AMD: a quantitative analysis. Br J Ophthalmol, 87:1159-1166.
[43] Luna G, Keeley PW, Reese BE, Linberg KA, Lewis GP, Fisher SK (2016). Astrocyte structural reactivity and plasticity in models of retinal detachment. Exp Eye Res, 150:4-21.
[44] Wang W, Min L, Qiu X, Wu X, Liu C, Ma J, et al. (2021). Biological Function of Long Non-coding RNA (LncRNA) Xist. Front Cell Dev Biol, 9:645647.
[45] Cheng Q, Wang L (2020). LncRNA XIST serves as a ceRNA to regulate the expression of ASF1A, BRWD1M, and PFKFB2 in kidney transplant acute kidney injury via sponging hsa-miR-212-3p and hsa-miR-122-5p. Cell Cycle, 19:290-299.
[46] Yang J, Qi M, Fei X, Wang X, Wang K (2021). Long non-coding RNA XIST: a novel oncogene in multiple cancers. Mol Med, 27:159.
[47] Chen F, Hu Y, Xie Y, Zhao Z, Ma L, Li Z, et al. (2020). Total Glucosides of Paeony Alleviate Cell Apoptosis and Inflammation by Targeting the Long Noncoding RNA XIST/MicroRNA-124-3p/ITGB1 Axis in Renal Ischemia/Reperfusion Injury. Mediators Inflamm, 2020:8869511.
[48] Xiao X, He Z, Tong S, Dai L, Xiao Q, Qin Z, et al. (2021). lncRNA XIST knockdown suppresses hypoxia/reoxygenation (H/R)-induced apoptosis of H9C2 cells by regulating miR-545-3p/G3BP2. IUBMB Life, 73:1103-1114.
[49] Zhang J, Chen C, Zhang S, Chen J, Wu L, Chen Z (2021). LncRNA XIST restrains the activation of Muller cells and inflammation in diabetic retinopathy via stabilizing SIRT1. Autoimmunity, 54:504-513.
[50] Yang LL, Li Q, Zhang X, Cao T (2020). Long non-coding RNA XIST confers aggressive progression via miR-361-3p/STX17 in retinoblastoma cells. Eur Rev Med Pharmacol Sci, 24:10433-10444.
[51] Xu C, Tian LH (2020). LncRNA XIST promotes proliferation and epithelial-mesenchymal transition of retinoblastoma cells through sponge action of miR-142-5p. Eur Rev Med Pharmacol Sci, 24:9256-9264.
[52] Cheng Y, Chang Q, Zheng B, Xu J, Li H, Wang R (2019). LncRNA XIST promotes the epithelial to mesenchymal transition of retinoblastoma via sponging miR-101. Eur J Pharmacol, 843:210-216.
[53] Wang Y, Sun D, Sheng Y, Guo H, Meng F, Song T (2020). XIST promotes cell proliferation and invasion by regulating miR-140-5p and SOX4 in retinoblastoma. World J Surg Oncol, 18:49.
[54] Yao L, Yang L, Song H, Liu TG, Yan H (2020). Silencing of lncRNA XIST suppresses proliferation and autophagy and enhances vincristine sensitivity in

retinoblastoma cells by sponging miR-204-5p. Eur Rev Med Pharmacol Sci, 24:3526-3537.

[55] Bhumika S, Lemmens K, Vancamp P, Moons L, Darras VM (2015). Decreased thyroid hormone signaling accelerates the reinnervation of the optic tectum following optic nerve crush in adult zebrafish. Mol Cell Neurosci, 68:92-102.

[56] Scheppke L, Aguilar E, Gariano RF, Jacobson R, Hood J, Doukas J, et al. (2008). Retinal vascular permeability suppression by topical application of a novel VEGFR2/Src kinase inhibitor in mice and rabbits. J Clin Invest, 118:2337-2346.

[57] Rowe-Rendleman CL, Durazo SA, Kompella UB, Rittenhouse KD, Di Polo A, Weiner AL, et al. (2014). Drug and gene delivery to the back of the eye: from bench to bedside. Invest Ophthalmol Vis Sci, 55:2714-2730.